Solid-State ^{19}F MAS, ^{19}F CRAMPS, and $^{19}F \rightarrow {}^{13}C$ CP/MAS NMR Study of an Amorphous Perfluoropolymer

Shinji Ando,*,† Robin K. Harris,‡ Jérôme Hirschinger,§ Stefan A. Reinsberg,‡,# and Ulrich Scheler⊥

Department of Organic and Polymeric Materials, Tokyo Institute of Technology, Ookayama, Meguro-ku, Tokyo, 152-8552, Japan; Department of Chemistry, University of Durham, South Road, Durham, DH1 3LE, UK; Institut de Chimie, UMR 7510, CNRS, Bruker S.A., Université Louis Pasteur, BP 296 67008 Strasbourg Cedex, France; and Institut für Polymerforschung, Dresden e.V., Postfach 120411, D-01005 Dresden, Germany

Received February 14, 2000

ABSTRACT: Solid-state ^{19}F high-speed MAS, ^{19}F CRAMPS, and $^{19}F \rightarrow {}^{13}C$ CP/MAS NMR spectra have been investigated for an amorphous fluoropolymer (CYTOP) having a five-membered heteroring in the main chain. In the ^{19}F MAS spectra, spinning at 35 kHz is necessary to ensure no spectral overlap of spinning sidebands (SSB) with the isotropic signals. The integrated areas obtained are consistent with the molecular structure, and the signal assignments were confirmed using shielding calculations by the GIAO method at a density functional level of theory, B3LYP/6-31G(d). A ^{19}F CRAMPS spectrum measured at a spinning speed of 6 kHz gives slightly narrower half-height widths despite SSB overlap. All fluorine signals show monoexponential decays in the ^{19}F spin-lock experiment with the same $T_{1\rho}^{F}$, indicating the structure is monophasic. Two fluorines connected to the same carbon give separate peaks at ambient temperature, which reflects the magnetic inequivalence at the axial and equatorial positions of the heteroring. However, they start to merge at 140 °C nominal temperature, which is explained by a conformational exchange caused by vigorous motion of the ring. $^{19}F \rightarrow {}^{13}C$ CP/MAS spectra of CYTOP were measured at a spinning speed of 6 kHz. The evolutions of the signal intensities in the $^{19}F \rightarrow {}^{13}C$ variable contact time CP experiments are adequately described by the quantum mechanical master equation applied to the three-spin CF_2 subsystem for the main peak and to the two-spin CF subsystems for the subpeak. The C−F distances and the time constants relating to the heteronuclear polarization transfer between ^{19}F and ^{13}C spins, those of the homonuclear effective spin-diffusion among fluorines and the decay or damping of the coherences, were obtained. In addition, the time constants of homonuclear spin diffusion among fluorines were independently measured by the ^{13}C-detected ^{19}F spin-diffusion experiment.

Introduction

There are a limited number of perfluoro-organic polymers (i.e., with no hydrogen in the molecular structures), and most of the conventional ones are semicrystalline (e.g., poly(tetrafluoroethylene) (PTFE), poly(tetrafluoroethylene-*co*-perfluoroalkylvinyl ether), and poly(tetrafluoroethylene-*co*-hexafluoropropylene) (FEP)). However, several amorphous perfluoropolymers that have heterocyclic structures in their main chain were developed in the 1980s.[1−4] These polymers exhibit conspicuous optical, electrical, and chemical properties. In particular, the very low refractive index (1.34 at a wavelength of 589 nm), the high optical transparency for a very wide range of wavelengths (from ultraviolet to near-infrared), and the good solubility in perfluorinated solvents cannot be obtained with semicrystalline perfluoropolymers.[5]

As has been reported, high-speed magic-angle spinning facilitates the measurement of high-resolution solid-state ^{19}F NMR spectra for partially fluorinated and perfluorinated polymers.[6−15] However, even if the repeating units of such conventional polymers have simple chemical structures, the semicrystalline nature (coexistence of crystalline and amorphous components), polymorphism in the crystalline components, and variations in regioregularity (head-to-head/tail-to-tail polymerized components) make their NMR spectra complicated. In addition, for polymers containing both hydrogen and fluorine, the heteronuclear polarization transfer between fluorines and protons makes the analyses of relaxation parameters and cross-polarization (CP) behavior among ^{13}C, ^{19}F, and ^{1}H nuclei complicated. Recently, we employed the phenomenological theory of spin thermodynamics based on the spin-temperature hypothesis to describe the polarization transfer between the ^{1}H and ^{19}F spin baths in an amorphous fluorinated polyimide and in a fluoroelastomer under MAS conditions.[16,17] Simultaneous fitting of the evolution of magnetization in the standard CP and a modified CP (TORQUE) experiment, using the exact solutions of the equations for the spin thermodynamics, gave unique sets of the parameters T_{HF}, $T_{1\rho}^{H}$, and $T_{1\rho}^{F}$.[17] A few applications of high-speed ^{19}F MAS NMR for perfluoropolymers have been published.[18] One article gave results from ^{19}F-MAS spectra of poly(tetrafluoroethylene), poly(tetrafluoroethylene-*co*-hexafluoropropylene), and their electron-beam-irradiated samples at spinning speeds up to 35 kHz.[14] In addition, oligomers of PTFE have been shown to give well-resolved spectra suitable for detailed structural analysis.[19] The same group has recently reported ^{19}F-MAS spectra of electron-beam-irradiated PTFE.[20] Cyclized perfluoropolymers are at-

† Tokyo Institute of Technology.
‡ University of Durham.
§ Université Louis Pasteur.
⊥ Institut für Polymerforschung.
Present address: Max-Planck-Institut für Polymerforshung, Ackermannweg 10, D-55128 Mainz, Germany.
* Corresponding author. Tel +81-3-5734-2137; Fax +81-3-5734-2889; E-mail sando@polymer.titech.ac.jp.

10.1021/ma000275z CCC: $20.00
Published on Web 12/08/2000

Scheme 1. Molecular Structure of CYTOP (a) and Its Possible Stereoisomers (b−d)[a]

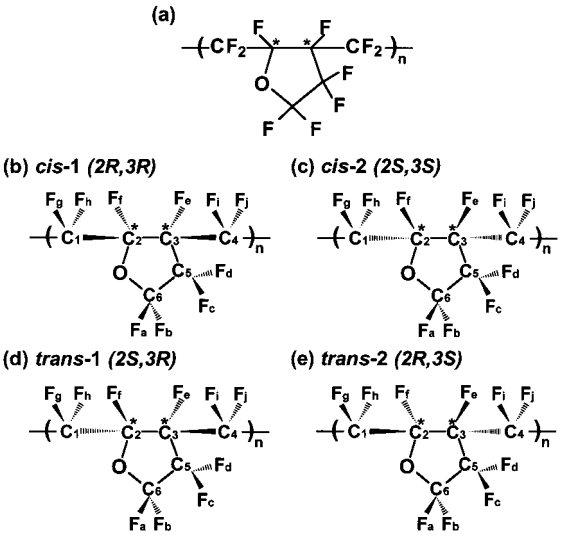

[a] Two chiral carbons in the main chain are marked by asterisks. The isomers are classified into two enantiomeric groups, *cis*- and *trans*-structures, based on the main-chain configuration (see text).

tractive materials for NMR investigation because most of the perfluoropolymers analyzed by ^{19}F MAS NMR so far are highly crystalline PTFE or fluoroelastomers that have very low glass transition temperatures (T_g). Only one attempt has been made to study an amorphous perfluoropolymer that has T_g higher than room temperature.[18]

We report here a solid-state ^{19}F MAS, ^{19}F CRAMPS, and ^{19}F → ^{13}C CP/MAS NMR investigation of an amorphous perfluoropolymer in a glassy state. This study should provide a further basis for the solid-state NMR analyses of insoluble and intractable fluoropolymers.

Experimental Section

Sample. The trade name of the cyclized perfluoropolymers used is CYTOP. They are synthesized by the polymerization of perfluoroalkenylvinyl ethers and are known to be completely amorphous perfluoropolymers, since the manufacturer reported that no crystalline peak is observed in wide-angle X-ray diffraction patterns.[21] The structure of the repeating unit of the polymer used in the present investigation is shown in Scheme 1a. A powdered sample obtained from the Asahi Glass Co. was used for the measurements after drying at 110 °C for 1 h (although this polymer has very low water absorption of less than 0.01%). The physical properties of the polymer have been reported in the literature,[21] but the molecular weight and its distribution, use of additives, and variation in the stereochemical structures are still unknown to us. A carbon content of 25.2% of the sample, determined by elemental analysis, is in agreement with the value calculated from the chemical structure (25.9%). Moreover, the glass transition temperature (T_g) of 108 °C, determined by DSC, coincides with the value reported by the manufacturer (107 °C) and suggests that the main chain is rigid at room temperature.

NMR Measurements. All the solid-state NMR work except for an ultrahigh-speed MAS experiment (≥25 kHz) was carried out on a Chemagnetics CMX-200 spectrometer operating at resonance frequencies of 188.288 and 50.328 MHz for fluorine and carbon nuclei, respectively. A commercial (Chemagnetics) ^{1}H−^{19}F double-tuned APEX MAS probe with 4 mm o.d. zirconia Pencil rotors was used for the ^{19}F spectra. Vespel drive tips, spacers, and end caps have been utilized to avoid unwanted background signal on the fluorine channel. To reduce the effect of inhomogeneity in the spin-locking field, two spacers (4 mm in length) were added to the ends of the sample. Thus, the actual sample length was about 3.5 mm. Samples were spun at the magic angle at rates of 6−16 kHz for the H−F probe. Experiments were carried out at ambient probe temperature except for the variable temperature measurement of ^{19}F MAS direct polarization (30−140 °C). We have reported that the calibrated ambient probe temperature inside the rotor was around 35 °C at a spin rate of 10 kHz.[17] Fluorine chemical shifts are quoted with respect to $CFCl_3$ (0 ppm) and were measured via a sample of liquid C_6F_6 (−164.3 ppm).

Single-pulse ^{19}F NMR spectra were recorded using direct polarization with $\pi/2$ pulses of 3 μs duration. Recycle delays of 10 s correspond to more than 5 times the spin−lattice relaxation time in the laboratory frame ($T_1^F = 1.8$ s). Variable-temperature (VT) ^{19}F MAS NMR spectra were taken by using the Chemagnetics temperature-control unit. Nitrogen was used as a VT gas. The measurements started 15 min after the temperature at the probe head reached the set value. This temperature was not calibrated to that inside the sample rotor. ^{19}F CRAMPS NMR spectra were recorded using the MREV-8 pulse sequence with $\pi/2$ pulses of 1.4 μs duration. A cycle time of 39 μs has been used successfully. Such a short cycle time allows spectral widths in excess of 250 ppm to be observed. The recycle delay for the CRAMPS experiment was 10 s, and the sample was spun at a rate of 6 kHz.

Carbon-13 NMR spectra were recorded following ^{19}F → ^{13}C CP with $\pi/2$ pulses of 5 μs duration for the fluorine nuclei using a triple-channel H−F−X probe at a spin rate of 6 kHz. The carbon and fluorine rf fields were adjusted to fulfill the first sideband matching condition: $|\omega_{1F}|/2\pi = 50$ kHz and $|\omega_{1C}|/2\pi = 44$ kHz. The Hartmann−Hahn matching condition was set using the sample (CYTOP). Free induction decays (FIDs) of the ^{13}C signals were acquired using high-power ^{19}F decoupling with a magnitude equivalent to about 47 kHz. ^{13}C chemical shifts were referenced by replacement against the high-frequency line of adamantane at 38.4 ppm relative to TMS. 7 mm o.d. zirconia Pencil rotors were used. Ceramic spacers, Vespel drive tips, and end caps have been utilized.

The pulse sequences used in this study are depicted in Figure 1. Fluorine spin−lattice relaxation times in the rotating frame ($T_{1\rho}^F$) were measured in the fluorine channel by variable ^{19}F spin-lock experiments using the H−F probe at spinning speeds of 16 kHz and in the carbon channel by variable ^{19}F spin-lock followed by short ^{19}F → ^{13}C CP (t_{CP} = 0.2 ms) experiments using the H−F−X probe at 6 kHz. The strength of the rf field used for spin-locking the fluorine nuclei was equivalent to 83 kHz for the H−F probe and 50 kHz for the H−F−X probe. The CP dynamics between the ^{19}F and ^{13}C nuclei were studied using the standard variable contact time CP experiment under the first sideband matching condition. The behavior of homonuclear spin diffusion among fluorines was separately measured by the pulse sequence of the ^{13}C-detected spin-diffusion (SD) experiment developed by Zhang et al.[22] Clearly, the ^{1}H capabilities of the two probes were not relevant for the present investigation.

The ultrahigh-speed MAS experiments (≥25 kHz) were carried out on a modified Bruker AMX 300 spectrometer operating at a resonance frequency of 282 MHz for fluorine nuclei. A Bruker BL2.5 CRAMPS probe head has been used. The samples were spun using 2.5 mm o.d. zirconia rotors, allowing for spinning frequencies of up to 35 kHz. The spectra were acquired using single-pulse excitation with a $\pi/2$ pulse duration of 3 μs, recycle delay of 4 s, spectral width of 125 kHz, and 128 transients. Fluorine chemical shifts are again quoted with respect to $CFCl_3$ but are measured via the CF_2 signal of PTFE (−122.0 ppm).

Shielding Constant Calculations. Calculations of ^{19}F and ^{13}C magnetic shielding constants were carried out using the ab initio molecular orbital (MO) computation package "Gaussian-94" (Revision E.2)[23] at the computer center of the University of Durham. Prior to the shielding constant calculations, the geometric structures of the model compounds were fully optimized using the density functional level of theory (DFT),

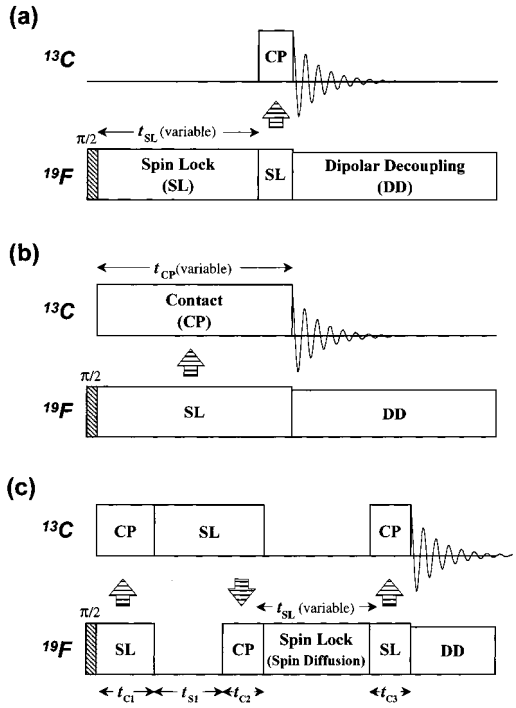

Figure 1. Pulse sequences for measuring parameters relevant to the cross-polarization (CP) dynamics between ^{19}F and ^{13}C: (a) ^{13}C-detected $T_{1\rho}^{F}$ measurement, (b) standard variable contact time (t_{CP}) CP, and (c) ^{13}C-detected spin-diffusion (SD) experiment.

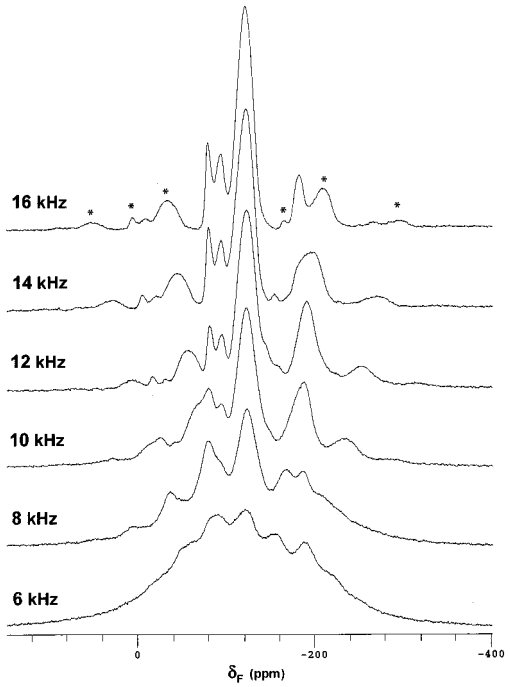

Figure 2. Solid-state ^{19}F MAS spectrum of CYTOP measured by direct polarization ($\pi/2$ pulse) at ambient probe temperature at different spinning rates in the range 6−16 kHz. Spectrometer operating conditions: fluorine $\pi/2$ pulse duration 3 μs, recycle delay 10 s, spectral width 200 kHz, and 32 transients. Peaks shown with asterisks are spinning sidebands.

B3LYP (Becke's three-parameter hybrid functionals), with an extended basis set of 6-31G(d). Fluorine-19 and carbon-13 shielding constants of the model compounds were calculated using gauge-including atomic orbitals (GIAO) at the same level of theory and with the same basis set.[24,25]

Results and Discussion

^{19}F MAS and ^{19}F CRAMPS Spectra. Since there are two chiral carbons in the main chain, the four kinds of stereoisomeric structures shown in Scheme 1b−e may be contained in CYTOP. These structures are classified into two enantiomeric groups based on the main-chain configuration, namely *cis*- and *trans*-structures. As shown in the figure, (*2R,3R*) (*cis*-1) and (*2S,3S*) (*cis*-2) are mutual enantiomers, and (*2S,3R*) (*trans*-1) and (*2R,3S*) (*trans*-2) also form an enantiomeric pair. The numbering of the fluorine and carbon atoms is also depicted in Scheme 1. Large local variations in configuration and conformation are likely to bring a highly amorphous nature to this polymer, although we have no information on the stereochemical structures.

At ambient temperature, significant homonuclear dipolar interactions among fluorines are expected in the solid state for this polymer because of the 100% natural abundance of ^{19}F and the very high fluorine content (68.3 wt %). In addition, large chemical shift anisotropies are sometimes exhibited by fluorines in organic molecules, which are comparable to those of ^{13}C atoms.[8,26] Hence, high-speed magic-angle spinning is required to reduce both the homonuclear dipolar interactions and the chemical shift anisotropy in order to observe high-resolution ^{19}F MAS spectra.

Figures 2 and 3 show the solid-state ^{19}F MAS spectra measured by direct polarization ($\pi/2$ pulse) with varying spinning rates between 6 and 35 kHz. The background signal of the probe is negligibly small because of the high fluorine content of the sample and the probe design involving low Teflon content. High-resolution spectra with separated signals were obtained at spinning speeds higher than 12 kHz. However, a part of the peak at −180.3 ppm is still overlapped at 16 kHz by the first spinning sideband (SSB) of the peak at −192.4 ppm. As will be described below, the dipolar interactions and the chemical shift anisotropy are unlikely to be completely averaged by MAS even at spin rates in excess of 16 kHz. Spinning at 35 kHz gives a spectrum completely free from the SSB-overlap problems, though one can still see spinning sidebands in the spectrum. Although the ^{19}F spectrum at 35 kHz does not give complete separation of the peaks, required for unambiguous signal assignments, it does give valid integration ratios for signal intensities. The results are as follows: the high-frequency signals (peak positions: −75.1 ppm, −89.8 ppm): 20.2%, the large central signal (−118.0 ppm): 69.8%, and the low-frequency signal (−177.7 ppm): 10.0%. Since the total number of fluorines in a repeating unit (Scheme 1) is 10, the ratio of the integrated intensities (2:7:1) can be directly attributed the number of fluorine atoms.

Figure 4 shows the ^{19}F solid-state CRAMPS spectrum of CYTOP measured using the MREV-8 pulse sequence at a spinning rate of 6 kHz (effectively 12.7 kHz). From the comparison with the MAS spectra, the overlap of a spinning sideband (arising from chemical shift anisotropy) can be seen to intensify the low-frequency signal resonating between −180 and −200 ppm. The sharp spikes appearing at −47, −105, −173, and −259 ppm are artifacts. Although the homonuclear dipolar interactions should be effectively suppressed by the multiple-pulse technique, the half-height width of the central signal (∼18 ppm) is close to those in the MAS spectra at high spinning rates (∼20 ppm at 35 kHz). This indicates that the main cause of the large half-height widths

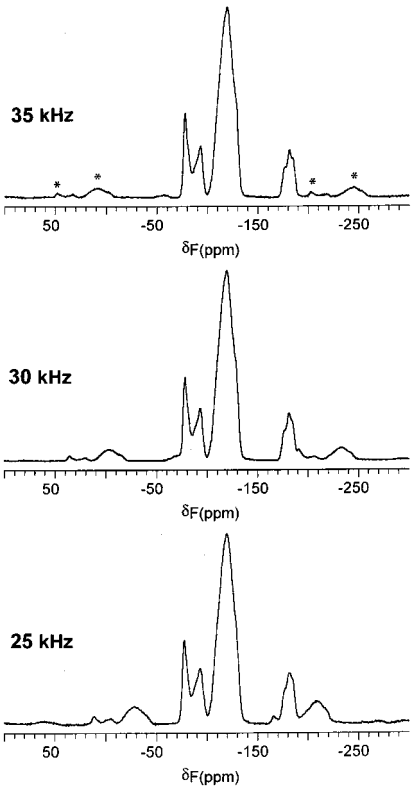

Figure 3. Solid-state ^{19}F ultrahigh-speed MAS spectrum of CYTOP measured by direct polarization (π/2 pulse) at ambient probe temperature at different spinning rates of 25−35 kHz. Spectrometer operating conditions: fluorine π/2 pulse duration 3 μs, recycle delay 4 s, spectral width 125 kHz, and 128 transients. Peaks shown with asterisks are spinning sidebands.

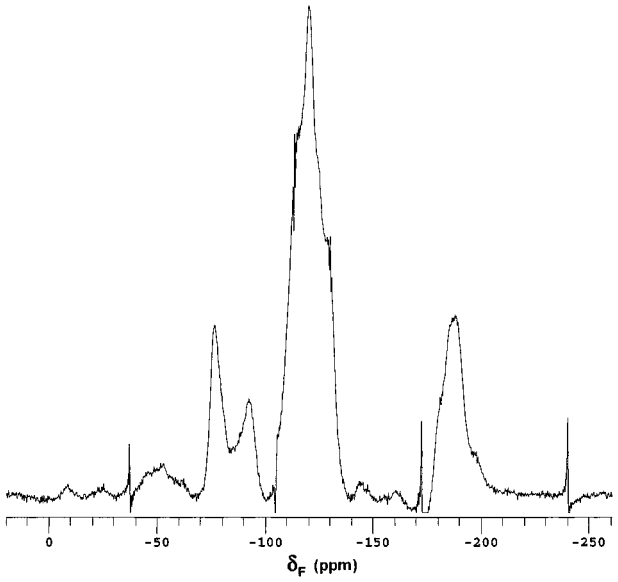

Figure 4. Solid-state ^{19}F CRAMPS spectrum of CYTOP measured using the MREV-8 pulse sequence at a spin rate of 6 kHz at ambient probe temperature. Spectrometer operating conditions for the spectrum: fluorine π-pulse duration 2.1 μs, cycle time 31.8 μs, recycle delay 10 s, and 32 transients.

of the signals in the MAS and CRAMPS spectra is not the residual F−F homonuclear dipolar interactions but the inherent chemical shift dispersion originating from the variety of configurations and conformations in CYTOP. Three "shoulders" are clearly observed on the left (−115 ppm) and right (−126 and −131 ppm) sides of the central signal in the CRAMPS spectrum, in contrast to its spectral similarity to the MAS spectra. This shows that the CRAMPS spectrum has better spectral resolution for the central signal, but it is difficult to assign these shoulder peaks (see below).

Scheme 2. Molecular Structure of 2-Substituted Perfluorooxolanes (PFO), the ^{19}F NMR Chemical Shifts of Which Have Been Reported in Ref 27[a]

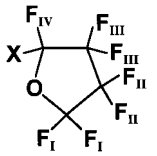

[a] The substituents, X, are $-CF_2CF_3$, $-CF_2CF_2CF_3$, $-CF_2CF_2Cl$, and $-CF(CF_3)\,CF_2CF_3$.

Table 1. ^{19}F Chemicals Shifts of 2-Substituted Perfluorooxolanes (PFO)[a]

	^{19}F chemical shift (ppm from $CFCl_3$)		
substituent (X)	F_I	F_{II} and F_{III}	F_{IV}
$-CF_2CF_3$	−86.9, −88.8	−127.7, −131.6, −130.5, −132.7[b]	−127.7
$-CF_2CF_2CF_3$	−82.3, −84.5	−121.4, −124.3, −127.0, −136.3	−124.0
$-CF_2CF_2Cl$	−85.2, −87.4	−119.8, −124.7, −129.0, −139.4, −131.3[b]	−125.2
$-CF(CF_3)CF_2CF_3$	−85.5 to −92.0[c]	−126.2 to −142.5[c]	−117.8

[a] The molecular structure is shown in Scheme 2, and the chemical shifts are taken from ref 27. [b] CF_2 signals of the substituent are included. [c] Overlapping signals.

The ^{19}F chemical shifts of 2-substituted perfluorooxolanes (PFO, Scheme 2) in the solution state, which have been reported by Grievson (Table 1), can be used to infer the signal assignments of the ^{19}F MAS and ^{19}F CRAMPS spectra of CYTOP.[27] The F_I fluorines in PFO always resonate at higher frequencies (−85 to −92 ppm) than the other fluorines attached to the heteroring (F_{II}, F_{III}, and F_{IV}: −120 to −143 ppm). In addition, the F_I signals are split into two peaks with chemical shift differences of ca. 2 ppm, and each F_I signal gives rise to AB-type patterns characterized by a *geminal* F−F coupling of ca. 130−140 Hz. From the comparison of the ^{19}F chemical shifts of CYTOP and PFO, the two signals which appear in the highest frequency region in the ^{19}F MAS spectra (−78 to −94 ppm) can be assigned to F_a and F_b despite the much larger peak separation of ca. 15 ppm. In addition, the other separate signal, in the lowest frequency region (−177 to −186 ppm), can be assigned to F_e because such a fluorine does not exist in PFO.

In the present study, quantum chemical calculations of magnetic shielding constants are used to confirm or determine the assignment of the signals in the solid-state ^{19}F and ^{13}C spectra. It has been reported that the Hartree−Fock and DFT(B3LYP) levels of theory with a relatively large basis set including polarization functions (e.g., 6-31G(d), 6-311G(d,p)) are applicable for predicting ^{13}C and ^{19}F chemical shifts of organic molecules.[25,28] Here, B3LYP/6-31G(d) was chosen for GIAO calculation of ^{19}F and ^{13}C magnetic shielding constants,[29] and four compounds were chosen as models for the calculation to reproduce the possible stereochemical structures of the repeating units (Scheme 1b−e**)**. Both ends of the models are capped by two trifluoromethyl ($-CF_3$) groups. Figure 5 shows schematic drawings of

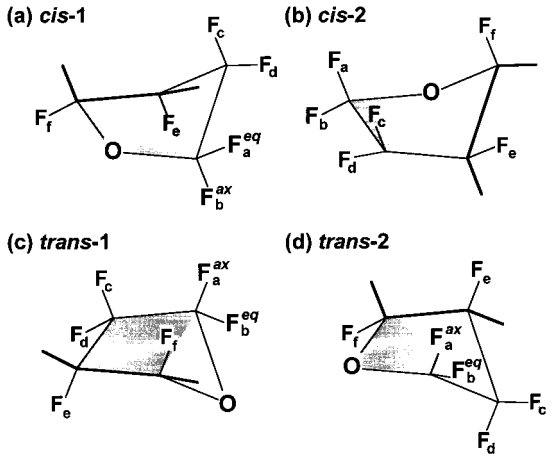

Figure 5. Schematic drawings of the optimized geometries of the heterorings for the four stereoisomeric model compounds. Four atoms in the five-membered ring are located almost in the same plane, and one of them is out of the plane for all the models. The fluorines located at the axial and equatorial positions are indicated as F^{ax} and F^{eq}, respectively.

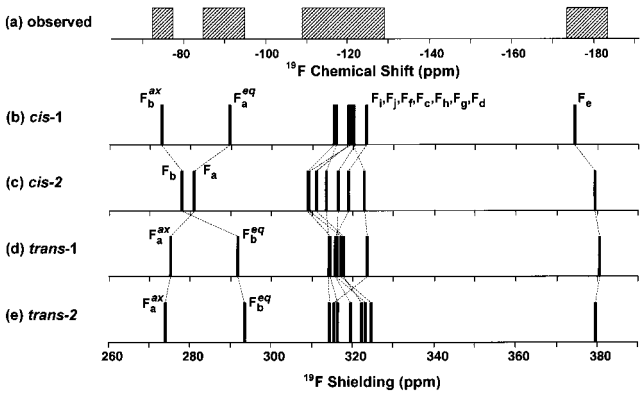

Figure 6. Schematic ^{19}F MAS spectrum of CYTOP (a) and stick spectra produced from the calculated ^{19}F shielding constants (b−e) of four model compounds (see text) using the DFT-GIAO theory. The relative positions between the experimental and calculated spectra are arbitrary.

the optimized geometric structures at the heterorings of the four stereoisomeric model compounds. It should be noted that each isomeric model exhibits different stereo-structures, but the optimized structure is not necessarily the unique conformation of the isomer. The optimized geometry might be changed by varying the initial structure used for the energy optimization. However, the important point to note is that the five-membered rings in all optimized structures have an "envelope conformation": four atoms are located almost in the same plane, but the fifth is out of the plane. Different atoms are out of the plane in each compound: C_5, C_2, O, and C_5 atoms are out of the plane in *cis*-1, *cis*-2, *trans*-1, and *trans*-2 structures, respectively. The variation of stereochemical structures could cause a large distribution in chemical shifts of fluorines and carbons in CYTOP. Figure 6 shows the schematic ^{19}F MAS spectrum of CYTOP (a) together with the stick spectra produced from the ^{19}F shielding constants (b−e) obtained using DFT-GIAO theory. In this figure, the relative positions between the experimental and the calculated spectra are arbitrary because calculated magnetic shielding constants are not easily converted to experimental chemical shifts. However, good agreement is observed between the experimental chemical shifts of CYTOP and the calculated ^{19}F shielding constants of the model compounds. Hence, the signal assignments of the F_a, F_b, and F_e fluorines described above are successfully confirmed, and the broad central signal (−118.0 ppm), with a large half-height width of 20 ppm, is assigned to other CF_2 fluorines (F_c, F_d, and F_f-F_i). The integrated intensities of the peaks measured at a spinning rate of 35 kHz agree well with the ratios of the three groups of fluorines in the molecular structure of CYTOP (Scheme 1), where 2:7:1 is the ratio of $(F_a + F_b):(F_c + F_d + F_f-F_i):F_c$. This also supports the validity of the signal assignments.

The shielding constants of F_a and F_b show interesting behavior depending on the molecular structure as seen in Figure 6. Although these two fluorines are connected to the same carbon (C_6), they show considerable difference in the experimental chemical shifts (14.7 ppm). In CYTOP, there are two major isomeric structures (*cis* and *trans* in the main chain), and the five-membered heterocyclic ring should not have planar structures. In addition, the exchange of such conformations should be prohibited or be much slower than the NMR time scale because the T_g of CYTOP (108 °C) is much higher than ambient probe temperature. Hence, they should have an "envelope" conformation, and F_a and F_b in CYTOP could be highly nonequivalent in the solid state at room temperature. The results of the calculations (Figure 6b,c,e) indicate that F_a and F_b in *cis*-1, *trans*-1, and *trans*-2 isomers are expected to resonate at separate positions, with chemical shift differences of ca. 15 ppm, in which one of the fluorines takes the equatorial (F^{eq}) and the other takes the axial position (F^{ax}) to the five-membered ring. This situation can be seen in Figure 5a,c,d. Hence, the signals resonating at −75.1 and −89.8 ppm can be assigned to the axial and equatorial fluorines, respectively. The large separation of the two peaks, F^{eq} and F^{ax}, at room temperature manifests the molecular rigidity at the heteroring, i.e., the absence of structural exchange between equatorial and axial positions. Similar phenomena have been observed in the ^{19}F NMR spectra of perfluorocyclohexane measured below −50 °C[30,31] and those of the equatorial and axial epimers of cyclohexylfluoride at −80 °C.[28] On the other hand, F_a and F_b in the *cis*-2 isomer are not expected to have significantly different ^{19}F chemical shifts because they take neither equatorial nor axial positions in the five-membered ring, as shown in Figure 5b. The electronic environment of these fluorines should be more symmetrical and similar to each other than those in the other isomers. The asymmetric shape of the two high-frequency signals (−78 to −94 ppm) can be ascribed to the overlap of peaks originating from the different isomeric structures. In particular, the two fluorines in the *cis*-2 isomeric structure can play an important role in distorting the split signals originating from the F_a and F_b fluorines of other isomeric structures. Further, the much smaller signal separation observed for the F_I fluorines in PFO in the liquid state results from the substantial averaging by molecular motion, i.e., interconversion of conformations, which should be faster than the NMR time scale at room temperature. The residual signal separation (∼2 ppm) reflects the inherent difference in the electronic environments between the two F_I fluorines close to and apart from F_{IV}. In other words, a much larger signal separation is expected for F_I fluorines when spectra are obtained at very low temperatures.

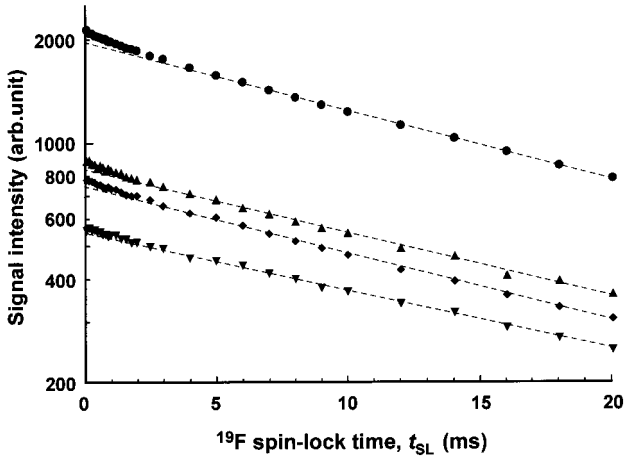

Figure 7. Spin-lock time dependence of ^{19}F signal intensities for four major peaks in the ^{19}F MAS spectra of CYTOP: ●, −120 ppm; ▲, −77 ppm; ◆, −92 ppm; ▼, −180 ppm. The plots were fitted by single-exponential functions, and the values of $T_{1\rho}^{F}$ thus obtained are identical for all the peaks within experimental error (23 ± 1 ms).

Moreover, the signal assigned to F_e, which appears in the most shielded region in the ^{19}F MAS spectra (−174 to −188 ppm in Figure 3), clearly shows overlapping features consisting of more than one component. In the spectrum measured at 35 kHz, one can see at least three components. This may also be attributed to the dependence of ^{19}F chemical shifts on the isomeric structures and their conformations. In other words, the separate peaks of F_a and F_b and the multiple components in the F_e signal manifest the molecular rigidity of CYTOP and the absence of site exchange at room temperature.

The other fluorines also show variations in the calculated magnetic shieldings. As described above, this can be primarily ascribed to the two major configurational structures, *cis* and *trans*. In addition, the combination of the variation in stereochemical structures in the main chain ((*R*,*R*) (*S*,*S*), (*R*,*S*), and (*S*,*R*)), that in the conformations at the heteroring structures, and that in the tacticity of the main chain, which accompanies different electronic environments in a polymer chain, can cause a distribution of ^{19}F chemical shifts. This could be the reason for the overlapping features in the MAS and CRAMPS spectra. Large distributions of ^{19}F chemical shifts should be more pronounced in amorphous polymers than in crystalline components in semicrystalline polymers.

^{19}F Spin−Lattice Relaxation Time in the Rotating Frame. Figure 7 shows the relaxation behavior of the four major peaks observed in the ^{19}F MAS spectra of CYTOP at a spinning rate of 16 kHz using the variable spin-lock time sequence at ambient probe temperature. Although a slightly faster relaxing component of less than 5% is observed at the shorter spin-lock times (t_{SL} < 3 ms), the decays of the peak intensities were fitted by single-exponential functions, and the spin−lattice relaxation times in the rotating frame ($T_{1\rho}^{F}$) thus obtained are identical for all the peaks within experimental error (23 ± 1 ms). We do not understand the origin of the small component, but we believe the major component is of principal interest and base our discussion on this. The value of $T_{1\rho}^{F}$ is as long as those of crystalline regions of semicrystalline polymers, which have low T_g's, such as poly(vinylidene fluoride)[10,11] and poly(vinyl fluoride),[32] measured under the same conditions. In the semicrystalline polymers, the crystalline phases generally show longer values of $T_{1\rho}^{F}$ by an order of magnitude compared with those of amorphous phases. The unique value of $T_{1\rho}^{F}$ for all the ^{19}F signals for CYTOP presumably arises from fast spin diffusion among fluorines, indicating that the fluorines are densely packed in the polymer chain and are tightly coupled with each other by homonuclear dipole−dipole interactions. When no molecular motion exists, the calculated nearest interatomic distances are less than 3 Å for all the fluorines, which supports this view. Since the chemical shift dispersion in the ^{19}F MAS spectra is more than 20 kHz (110 ppm), and the signals assigned to F_a, F_b, and F_e fluorines are separate from the large central peak, the spectral spin diffusion between these fluorines is not expected to be so effective. The spin−lattice relaxation times in the laboratory frame (T_1^F) are also well fitted by a single-exponential function and identical for all the signals (1.8 ± 0.1 s). These facts coincide with the uniphase amorphous nature and the absence of vigorous molecular motion in the polymer chains at ambient temperature.

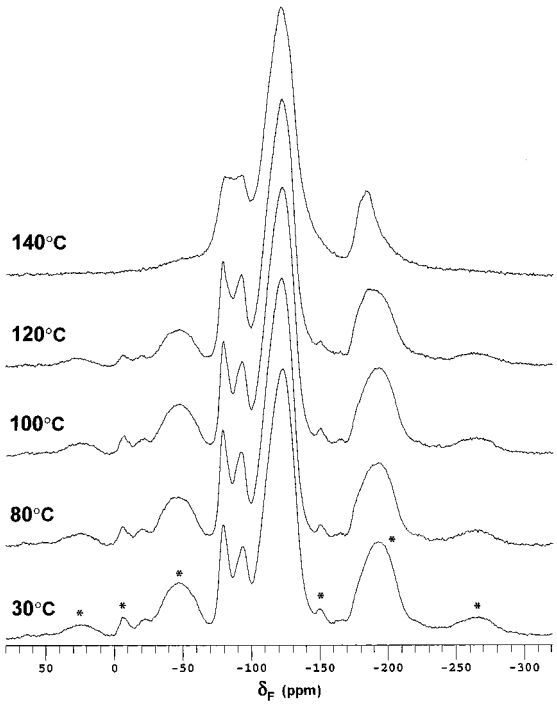

Figure 8. Solid-state ^{19}F MAS spectrum of CYTOP measured by direct polarization (π/2 pulse) at spin rates of 13.4−14.0 kHz at different set temperatures between 30 and 140 °C. The spectrometer operating conditions are the same as in Figure 2.

^{19}F MAS Spectra at Elevated Temperatures. Figure 8 shows the solid-state ^{19}F MAS spectra of CYTOP at spinning rates of 13.4−14.0 kHz with variations of the set temperature between 30 and 140 °C. There is no significant change in the spectra below 100 °C. A slight change in the shape of the peak at −180.3 ppm is caused by displacement of a spinning sideband resulting from an unexpected increase in spinning speed at the elevated temperatures. Subsequently, the high-frequency signals assigned to F_a and F_b start to merge (the valley between the two peaks becomes shallow) above 100 °C, which is accentuated considerably at 140 °C. It looks as if the averaging starts above T_g (108 °C). The peak to peak difference is decreased to 11.0 ppm

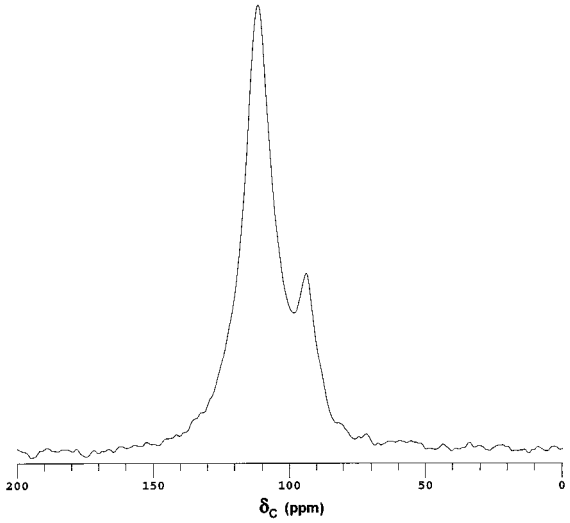

Figure 9. Solid-state $^{19}F \rightarrow {}^{13}C$ CP/MAS spectrum of CYTOP measured at a spinning speed of 6 kHz at ambient probe temperature. The contact time used was 1 ms, and the fluorine spins were decoupled during acquisition.

at 140 °C, which suggests that a considerable molecular motion occurs at the ring. The most probable motion is a fast puckering of the five-membered ring ("envelope" flapping). In principle, no motion can make F_a and F_b equivalent for the *cis*-forms because of the structural relationships of the main chain to them. No exact equivalence of F_a and F_b can be obtained for the *trans*-forms because the interactions between F_a and F_f are not identical to those between F_b and F_e. However, this molecular motion can reduce the chemical shift difference between F_a and F_b, in which two fluorines become magnetically similar by the fast structural exchange between the equatorial and axial positions. Moreover, the intensities of the spinning sidebands become very weak at 140 °C. The average anisotropy of calculated nuclear shielding tensors ($|\sigma_{11} - \sigma_{33}|$) for all the fluorines is about 115 ppm, which correspond to 22 kHz at the resonant frequency of fluorine. The smallest value of ca. 50 ppm is obtained for F_e, and the largest values of ca. 130 ppm are obtained for F_c and F_i. Further, the homonuclear dipolar interactions between the fluorines $(\mu_0/4\pi)(\hbar/2\pi)(\gamma_F{}^2/r^3)$ in a CF_2 group is about 16 kHz, where the optimized F−F distance is ca. 2.14 Å in the models. Hence, neither the chemical shift anisotropy nor the dipolar interactions should be completely averaged at ambient temperature by a spin rate of ca. 14 kHz. However, the molecular motion at 140 °C considerably reduces the chemical shift anisotropy and the dipolar interactions, with the aid of MAS at 14 kHz, as is revealed by the disappearance of SSB. After the measurement, the sample taken out from the rotor was a fused lump and looked translucent. Although no softening temperature has been reported for this polymer, fusion of fine particles is thought to occur at elevated temperatures above T_g.

$^{19}F \rightarrow {}^{13}C$ CP MAS Spectra. Figure 9 shows the $^{19}F \rightarrow {}^{13}C$ CP/MAS spectrum of CYTOP measured at ambient probe temperature at a spinning speed of 6 kHz. The contact time used was 1 ms, and the fluorine channel was subsequently irradiated with a power equivalent to 47 kHz during signal acquisition. Although little spectral resolution is observed, a small signal (subpeak) is distinctly seen on the low-frequency side of the major signal (main peak). The ^{13}C chemical shifts of the main peak and subpeak are 111.4 and 93.4 ppm, respectively. The line shapes of both peaks are well fitted by single Lorentzian functions, and the ratio of the integrated signal intensity of the main peak to that of the subpeak is 5:1.

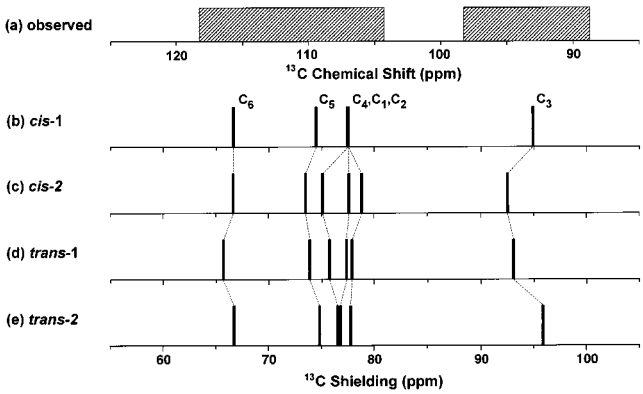

Figure 10. Schematic ^{13}C CP/MAS spectrum of CYTOP (a) and stick spectra produced from the calculated ^{13}C shielding constants (b−e) using the DFT-GIAO theory. The relative positions between the experimental and calculated spectra are arbitrary. The subpeak resonating at 93.4 ppm in Figure 9 is straightforwardly assigned to C_3.

Figure 10 shows the schematic ^{13}C spectrum of CYTOP (a) together with the stick spectra depicted from the calculated ^{13}C shielding constants using ab initio DFT-GIAO theory (b−e). The half-height widths of the observed signals are used for the drawing of (a). The relative positions between the experimental and calculated spectra are arbitrary, as described above. From the comparison between (a) and (b−e), the subpeak resonating at 93.4 ppm is straightforwardly assigned to that of C_3. The significant low-frequency displacement for this carbon from the others can be explained by its tertiary nature (−CF−), while the signal for the other tertiary C_2 carbon is displaced to high frequency due to the influence of the adjacent oxygen. All the carbons except for C_3 give rise to the broad main peak with a large half-height width of 14.1 ppm, whereas the half-height width of the subpeak is 6.7 ppm. Although signal intensity obtained from CP measurement does not necessarily reflect the chemical composition, the same ratio of integral intensity of the major to the subpeaks (5:1) was obtained between $t_{CP} = 0.5$ and 3 ms, and this value coincides with the number of carbons in the repeating unit of CYTOP: five carbons (C_1, C_2, and C_4−C_6) versus one carbon (C_3). As explained for the ^{19}F spectra, the variations in configurational and conformational molecular structures of CYTOP can cause large distributions of ^{13}C chemical shifts. Although the spin rate (6 kHz) is much lower than that for the ^{19}F spectra (16−35 kHz), the heteronuclear dipolar interactions between F and C are effectively suppressed by the broad-band ^{19}F decoupling during acquisition. Since no spinning sidebands are observed in the spectrum, the chemical shift anisotropy is effectively averaged at this spinning rate for all the carbons. The average anisotropy of the calculated ^{13}C nuclear shielding tensors ($|\sigma_{11} - \sigma_{33}|$) for all carbons in the models is about 17 ppm, corresponding to 850 Hz at the resonant frequency of carbon. The smallest value of ca. 9−14 ppm is for C_2, and the largest value of 24−26 ppm is for C_3. It should be noted that these values of the anisotropies are much smaller than those of the fluorines discussed above.

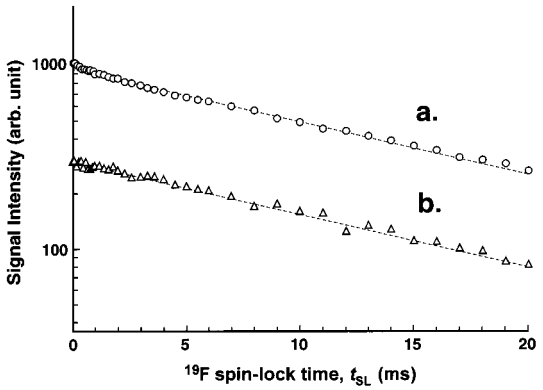

Figure 11. Spin-lock time dependence of ^{13}C peak intensities for two major signals of CYTOP (○, 112 ppm; △, 93 ppm), obtained using the pulse sequence shown in Figure 12a. A contact time of 0.1 ms and 64 transients were used for the indirect measurement of $T_{1\rho}^{F}$. The plots were fitted by single-exponential functions, and the values of $T_{1\rho}^{F}$ thus obtained are identical for both peaks within experimental error (17.5 ± 1 ms).

Figure 11 shows the decays of ^{19}F magnetization as detected indirectly by variable ^{19}F spin-lock followed by short ^{19}F → ^{13}C CP (t_{CP} = 0.2 ms) experiments as a function of the spin-lock time, t_{SL}. Both curves are well fitted by single-exponential functions, and the indirectly measured $T_{1\rho}^{F}$ (via ^{13}C resonance) is 17.5 ms for both signals. This also supports the uniphase amorphous nature and the absence of vigorous molecular motion in CYTOP. The relatively short value of $T_{1\rho}^{F}$ compared to the directly measured values in the ^{19}F spectra primarily arises from the difference in the spin-locking fields (83 kHz for the ^{19}F observation and 50 kHz for the ^{13}C observation).

Cross-Polarization Behavior for ^{19}F → ^{13}C CP. Figure 12 shows the evolution of signal intensities for the main peak and subpeak in the ^{13}C CP/MAS NMR spectra as a function of contact time, t_{CP}. The heights of each deconvoluted Lorentzian function were used as respective signal intensities, for which the half-height widths were fixed. In the initial period of the CP, the polarization oscillates between the *I* (fluorine-19) and *S* (carbon-13) spins with a frequency related to the magnitude of the heteronuclear dipolar coupling (Figure 12a,c). In this study, the cross-polarization dynamics were analyzed using density matrix calculations that have been used previously to account for the spin dynamics between ^{13}C and ^{1}H spins in organic compounds and polymers.[33] The CF_2 and CF spin systems in CYTOP can be treated as tightly coupled CF_n (n = 1, 2) groups immersed in a thermal bath consisting of the remaining fluorines. Neglecting $T_{1\rho}$ relaxation, the reduced density operator σ describing the CF_n subsystem evolves under the quantum mechanical master equation.[34]

$$\frac{d}{dt}\sigma(t) = -i[H(t),\sigma(t)] - \Gamma[\sigma(t) - \sigma(\infty)] \qquad (1)$$

where the spin Hamiltonian $H(t)$ is expressed in the "doubly rotating" interaction frame as a sum over the time-independent *I*-spin and *S*-spin rf field terms and the MAS-modulated hetero- and homonuclear dipolar coupling terms (resonance offsets are neglected).[33] The phenomenological isotropic spin-diffusion superoperator Γ that brings the *n* directly bound *I*-spin(s) into thermal equilibrium with the reservoir of the remaining fluorines with a rate *R* is represented by[34]

$$\Gamma(\sigma) = \sum_{k=1}^{n} R\{[I_{kx},[I_{kx},\sigma]] + [I_{ky},[I_{ky},\sigma]] + [I_{kz},[I_{kz},\sigma]]\} \qquad (2)$$

The expression of the *S*-spin magnetization is given by

$$S(t) = \mathrm{Tr}[\sigma(t)S_x] \qquad (3)$$

Two different rate constants, $R_{dp} = 1/T_{dp}$ and $R_{df} = 1/T_{df}$, can be introduced into Γ, in which T_{dp} only acts on the decay or damping of the coherences and T_{df} only controls the "effective" spin-diffusion process.[33,35]

As shown in Figure 12b,d, the evolutions of the signal intensities are adequately described by eq 1 applied to the three-spin CF_2 (n = 2) subsystem for the main peak and to the two-spin CF (n = 1) subsystem for the subpeak. The fitting was carried out for the initial period of the CP (t_{CP} < 1.0 ms) so that $T_{1\rho}$ relaxation may be safely neglected. In the calculation, the carbon and fluorine rf fields were fixed to fulfill the first sideband matching condition, $|\omega_{1F}|/2\pi$ = 50 kHz and $|\omega_{1C}|/2\pi$ = 44 kHz, as for the experimental work. Note that the superoperator Γ is expected to provide an adequate description of the cross-polarization dynamics because the existence of a secular (time-independent) heteronuclear flip-flop term at the first- and second-order sidebands leads to the same (quasi-)equilibrium states as for the static case at the Hartmann−Hahn match ($\omega_{1F} = \omega_{1C}$). The results thus obtained are r_{CF} = 1.38 ± 0.02 Å, T_{dp} = 220 ± 20 μs, and T_{df} = 1.6 ± 0.1 ms for the main-peak and r_{CF} = 1.42 ± 0.02 Å, T_{dp} = 180 ± 20 μs, and T_{df} = 2.5 ± 0.1 ms for the subpeak, where r_{CF} is the effective C−F distance. The angle formed by two C−F bonds in the CF_2 groups (F−C−F) was fixed to the tetrahedral angle (109.5°) in the optimization procedure. Since the main peak consists of the overlap of four CF_2 (C_1, C_4, C_5, C_6) signals and one CF (C_2) signal, the assumption n = 2 may be acceptable.

The average C−F distances in the optimized geometries calculated for the four model compounds are 1.352, 1.366, 1.372, 1.351, 1.345, and 1.340 Å for the F_g−C_1−F_h, C_2−F_f, C_3−F_e, F_i−C_4−F_j, F_c−C_5−F_d, and F_a−C_6−F_b components, respectively. The C_3−F_e bond is significantly longer (by 0.23 Å) than the average value for the other C−F bonds (1.349 Å), which is presumably reflected in the experimental values of the C−F distances. Although the C−F distances obtained from the CP dynamics are slightly longer than the values from geometry optimization, these facts indicate that there is no significant molecular motion that would average heteronuclear dipolar interaction between carbons and directly bonded fluorines. The average F−C−F angle in the optimized geometries is 108.9°. In contrast, the C−H dipolar coupling constant of 3.0 kHz in poly(trifluoroethylene) (PTrFE), observed in a ^{1}H → ^{13}C inversion−recovery CP experiment at ambient temperature, is considerably smaller than the expected value of 8.0 kHz for average C−H distances (1.1 Å).[36,37] This can be ascribed to a sizable molecular motion that leads to a scaling factor of ca. $^{2}/_{5}$ for the magnitude of dipolar coupling.

The homonuclear spin-diffusion time T_{df} for the main peak (1.6 ms) is significantly shorter than that of the

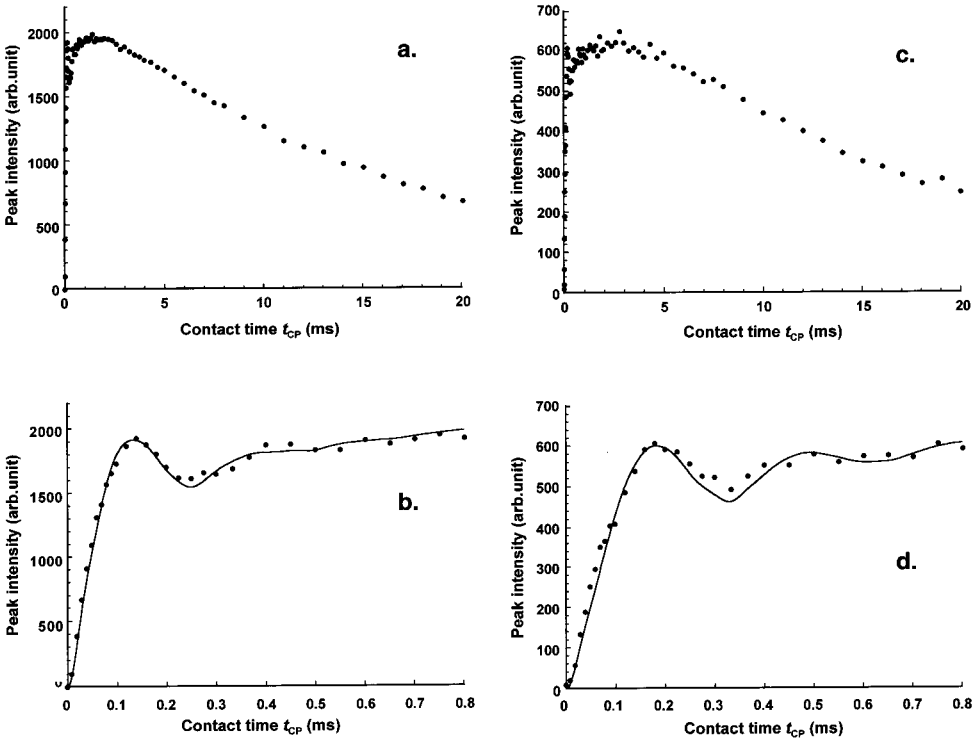

Figure 12. Contact time dependence of signal intensities for the $^{19}F \rightarrow {}^{13}C$ CP/MAS experiment on CYTOP using the pulse sequence shown in Figure 12b: (a) the evolution of the main peak (112 ppm), (b) an expansion of (a) at the initial stage, (c) the evolution of the subpeak (93 ppm), and (d) an expansion of (c). The fitted curves using eq 3 are also incorporated.

subpeak (2.5 ms). This principally originates from the spectral spin diffusion that is due to the overlap of signals, but the mutual proximity of fluorines in neighboring CF_2 groups also promotes spin diffusion. On the other hand, C_3-F_e is relatively separate from the other groups both in the molecular structure (Scheme 1 and Figure 5) and in the ^{19}F MAS spectrum (Figure 3). In addition, the time constant T_{dp} for the main peak (220 μs) is longer than that of the subpeak (160 μs). Although T_{dp} should be of the order of T_2, the transient oscillations are invariably damped by rf field inhomogeneities and heteronuclear dipolar interactions of the *S*-spin with more remote *I*-spins.[35] Hence, no reliable interpretation can be made for the difference in T_{dp} between the two peaks.

Spin-Diffusion between Fluorines Detected by ^{13}C. The time constant for spin diffusion among fluorines can be independently measured by the ^{13}C-detected ^{19}F spin-diffusion experiment. The pulse sequence is shown in Figure 1c. The first contact time (t_{C1}) was 1 ms, and the second and third contact times (t_{C2} and t_{C3}) were 0.1 ms. During t_{S1}, the magnetization of the fluorines decays to zero because t_{S1} (=1 ms) is chosen to be much larger than the time constant T_2 of the fluorine FID. The time t_{C2} should be sufficiently shorter than the spin-diffusion time in order to polarize only the fluorines directly connected to ^{13}C. After the second CP in this sequence, only the fluorines directly connected to ^{13}C are polarized, and they are spin-locked by the subsequent irradiation. During the spin-lock time (t_{SL}), a certain part of the fluorine magnetization diffuses to the neighboring fluorines, and thus the decaying time constant (T_D) represents the rate of spin diffusion among fluorines. Figure 13 shows the decays of ^{13}C magnetization observed in the variable ^{19}F spin-diffusion time followed by a short $^{19}F \rightarrow {}^{13}C$ CP. The spin-diffusion time (T_{SL}) was varied between 0.01 and 1.2

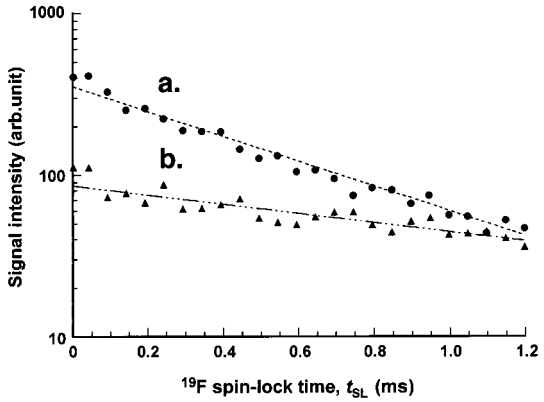

Figure 13. Spin-diffusion time dependence of ^{13}C signal intensities for the two major signals of CYTOP (●, 112 ppm; ▲, 93 ppm) using the pulse sequence shown in Figure 12c. The first contact time was 1 ms, and the second and third contact times were 0.1 ms. The spectral shape is the same as in Figure 9.

ms. The decay time constant T_D obtained for the main peak (0.56 ms) is significantly shorter than that for the subpeak (1.49 ms). This agrees with the T_{df} observed in the variable contact time CP experiment. This confirms that the spin diffusion of the F_e fluorines is slower than that of the other fluorines.

Conclusion

Fluorine-19 MAS spectra of an amorphous fluoropolymer having a five-membered heteroring in the main chain (CYTOP) show good spectral resolution at a spin rate of 35 kHz, without spectral overlap of spinning sidebands. The integrated intensities of the signals coincide with the number of fluorines in the repeat unit. A similar ^{19}F spectrum was obtained by the CRAMPS technique with slightly higher resolution. All the fluo-

rine signals show identical values of $T_{1\rho}^{F}$ that are similar to those observed for the crystalline components of fluorovinyl polymers, which supports a homogeneous phase structure and absence of vigorous molecular motion at ambient temperature. Two separate signals resonating in the high-frequency region are assigned to two fluorines that are connected to the same carbon, but they start to merge at 140 °C VT gas temperature. This is explained by a conformational exchange originating from molecular motion at the heteroring occurring above T_g. The homonuclear dipolar interactions among fluorines and chemical shift anisotropies of fluorine atoms are also averaged at this temperature with the help of MAS at 14 kHz. The contact time dependencies of signal intensities in $^{19}F \rightarrow {}^{13}C$ CP/MAS spectra are adequately described by a theoretical approach based on the quantum mechanical master equation, including the processes of coherent magnetization transfer between ^{19}F and ^{13}C and homonuclear spin diffusion among fluorines. The equations used for the fittings were applied to the three-spin CF_2 ($n = 2$) subsystem for the main peak and to the two-spin CF ($n = 1$) subsystem for the subpeak. The effective C−F distances obtained through the dipolar oscillation frequencies of the main peak and subpeak are comparable to the average values obtained from ab initio calculations at a density functional level of theory (B3LYP/6-31G(d)), indicating that the heteronuclear dipolar interactions are not averaged by molecular motion. This coincides with the fact that the T_g of CYTOP is much higher than ambient temperature. The time constant of homonuclear spin-diffusion among fluorines (T_{df}) obtained for the main peak is significantly shorter than that of the subpeak. This agrees with the results of the ^{13}C-detected spin-diffusion (SD) experiments. Larger values of T_{df} and T_D for the C_3 carbon than those of the other carbons may arise from the decreased spectral spin-diffusion for the F_e fluorine which resonates in the most shielded region of the ^{19}F MAS spectra. Solid-state ^{19}F high-speed MAS, ^{19}F CRAMPS, and $^{19}F \rightarrow {}^{13}C$ CP/MAS NMR spectra are useful methods for analyzing chemical structures and obtaining parameters relating to molecular motion, CP dynamics, and spin diffusion in amorphous perfluoropolymers.

Acknowledgment. S.A. is grateful to the Japan Society for the Promotion of Science for a research fellowship in the UK. J.H. is grateful to the Royal Society of Great Britain for a study visit under the European Science Exchange Program. We also thank B. J. Say, A. M. Kenwright, and P. Holstein for helpful discussions. Financial support from the UK Engineering and Physical Sciences Research Council under Grant GR/L02906 is gratefully acknowledged.

References and Notes

(1) Nakamura, M. US Patent 4,897,457, 1990.
(2) Nakamura, M.; Kawasaki, T.; Unoki, M.; Oharu, K.; Sugiyama, N.; Kojima, G. *Progress in Pacific Polymer Science*; Springer-Verlag: Berlin, 1991; p 369.
(3) Resnick, P. R. *Polym. Prepr. (Am. Chem. Soc., Div. Polym. Chem.)* **1990**, *31*, 312.
(4) Buck W. H.; Resnick, P. R. Electrochemical Society, Spring Meeting, Honolulu; Ext. Abs. **1993**, *93−1*, 548.
(5) Sugiyama, N. *Polym. Prepr. (Am. Chem. Soc., Div. Polym. Chem.*) **1998**, *39*, 1028.
(6) Dec, S. F.; Wind, R. A.; Maciel, G. E.; Anthonio, F. E. *J. Magn. Reson.* **1986**, *70*, 355.
(7) Dec, S. F.; Wind, R. A.; Maciel, G. E. *Macromolecules* **1987**, *20*, 2754.
(8) Harris, R. K.; Jackson, P. *Chem. Rev.* **1991**, *91*, 1427.
(9) Holstein, P.; Scheler, U.; Harris, R. K. *Magn. Reson. Chem.* **1997**, *35*, 647.
(10) Holstein, P.; Scheler, U.; Harris, R. K. *Polymer* **1998**, *39*, 4937.
(11) Holstein, P.; Harris, R. K.; Say, B. J. *Solid State Nucl. Magn. Reson.* **1997**, *8*, 201.
(12) Scheler, U.; Harris, R. K. *Chem. Phys. Lett.* **1996**, *262*, 137.
(13) Scheler, U.; Harris, R. K. *Solid State Nucl. Magn. Reson.* **1996**, *7*, 11.
(14) Scheler, U. *Solid State Nucl. Magn. Reson.* **1998**, *12*, 9.
(15) Isbester, P. K.; Kestner, T. A.; Munson, E. J. *Macromolecules* **1998**, *31*, 8192.
(16) Ando, S.; Harris, R. K.; Reinsberg, S. A. *J. Magn. Reson.* **1999**, *141*, 91.
(17) Ando, S.; Harris, R. K.; Monti, G. A.; Reinsberg, S. A. *Magn. Reson. Chem.* **1999**, *37*, 709.
(18) Legeay, G.; Coudreuse, A.; Legeais, J.; Werner, L.; Bulou, A.; Buzare, J.; Emery, J.; Silly, G. *Eur. Polym. J.* **1998**, *34* 1457.
(19) Katoh, E.; Sugimoto, H.; Kita, Y.; Ando, I. *J. Mol. Struct.* **1995**, *355*, 21.
(20) Katoh, E.; Sugisawa, H.; Oshima, A.; Tabata, Y.; Seguchi, T.; Yamazazki, T. *Radiat. Phys. Chem.* **1998**, *54*, 165.
(21) Aosaki, K. *J. Soc. Hybrid Microelectron. (Jpn.)* **1996**, *12*, 2.
(22) Zhang, S.; Meier, B. H.; Ernst, R. R. *Solid State Nucl. Magn. Reson.* **1992**, *1*, 313.
(23) Frisch, M. J.; Trucks, G. W.; Schlegel, H. B.; Gill, P. M. W.; Johnson, B. G.; Robb, M. A.; Cheeseman, J. R.; Keith, T.; Petersson, G. A.; Montgomery, J. A.; Raghavachari, K.; Al-Laham, M. A.; Zakrzewski, V. G.; Ortiz, J. V.; Foresman, J. B.; Cioslowski, J.; Stefanov, B. B.; Nanayakkara, A.; Challacombe, M.; Peng, C. Y.; Ayala, P. Y.; Chen, W.; Wong, M. W.; Andres, J. L.; Replogle, E. S.; Gomperts, R.; Martin, R. L.; Fox, D. J.; Binkley, J. S.; Defrees, D. J.; Baker, J.; Stewart, J. P.; Head-Gordon, M.; Gonzalez, C.; Pople, J. A. *Gaussian 94*, revision E.2; Gaussian, Inc.: Pittsburgh, PA, 1995.
(24) Wolinski, K.; Hinton, J. F.; Pulay, P. *J. Am. Chem. Soc.* **1990**, *112*, 8251.
(25) Cheeseman, J. R.; Trucks, G. W.; Keith, T. A.; Frisch, M. J. *J. Chem. Phys.* **1996**, *104*, 5797.
(26) Harris, R. K.; Jackson, P.; Nesbett, G. J. *J. Magn. Reson.* **1989**, *85*, 294.
(27) Grievson, B. Ph.D. Thesis, University of Durham, 1983.
(28) Adcock, W.; Lünsmann, D.; Peralta, J. E.; Contreras, R. H. *Magn. Reson. Chem.* **1999**, *37*, 167.
(29) The "d" in 6-31G(d,p) indicates that d-type polarization functions are located on atoms except for hydrogen, and the "p" indicates that p-type functions are on hydrogens. Hence, 6-31G(d,p) and 6-31G(d) are the same basis sets for perfluorinated organic molecules because of the absence of hydrogens.
(30) Homer, J.; Thomas, L. F. *Trans. Faraday Soc.* **1963**, *59*, 2431; **1966**, *62*, 2980.
(31) Homer, J.; Thomas, L. F. *Proc. Chem. Soc.* **1961**, 139.
(32) Ando, S.; Harris, R. K.; Holstein, P.; Reinsberg, S. A., to be submitted.
(33) Reinheimer, P.; Hirschinger, J.; Gilard, P.; Goetz, N. *Magn. Reson. Chem.* **1997**, *35*, 757.
(34) Müller, L.; Kumar, A.; Baumann, T.; Ernst, R. R. *Phys. Rev. Lett.* **1974**, *32*, 1402.
(35) Hirschinger, J.; Hervé, M. *Solid State Nucl. Magn. Reson.* **1994**, *3*, 121.
(36) Reinsberg, S. A. M.Sc. Thesis, University of Durham, 1998.
(37) Reinsberg, S. A.; Ando, S.; Harris, R. K. *Polymer* **2000**, *41*, 3729.

MA000275Z